THE JOURNAL OF PHYSICAL CHEMISTRY A
A JOURNAL OF THE AMERICAN CHEMICAL SOCIETY

pubs.acs.org/JPCA

Article

Core and Valence Level Photoelectron Spectroscopy of Nanosolvated KCl

Eetu Pelimanni,* Lauri Hautala, Andreas Hans, Antti Kivimäki, Mati Kook, Catmarna Küstner-Wetekam, Lutz Marder, Minna Patanen, and Marko Huttula

Cite This: *J. Phys. Chem. A* 2021, 125, 4750–4759

Read Online

ACCESS | Metrics & More | Article Recommendations | Supporting Information

ABSTRACT: The solvation of alkali and halide ions in the aqueous environment has been a subject of intense experimental and theoretical research with multidisciplinary interests; yet, a comprehensive molecular-level understanding has still not been obtained. In recent years, electron spectroscopy has been increasingly applied to study the electronic and structural properties of aqueous ions with implications, especially in atmospheric chemistry. In this work, we report core and valence level (Cl 2p, Cl 3p, and K 3p) photoelectron spectra of the common alkali halide, KCl, doped in gas-phase water clusters in the size range of a few hundred water molecules. The results indicate that the electronic structure of these nanosolutions shows a distinct character from that observed at the liquid–vapor interface in liquid microjets and ambient pressure setups. Insights are provided into the unique solvation properties of ions in a nanoaqueous environment, emerging properties of bulk electrolyte solutions with growing cluster size, and sensitivity of the electronic structure to varying solvation configurations.

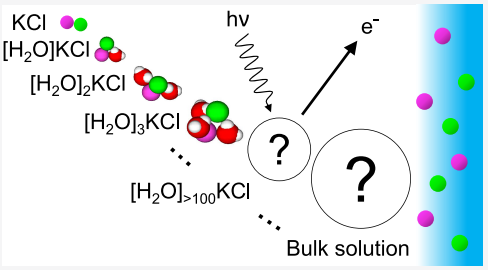

INTRODUCTION

Aqueous alkali and halide ions are involved in a myriad of natural and technological processes, yet their structural and electronic properties are not fully understood. Clusters play a central role in probing the detailed interplay of ions with water molecules, in both experiments and theory.[1−6] Clusters can be considered as simplified models of bulk solutions, but they are also in many ways unique as the solvation structures and dynamics are subject to, e.g., the high surface-to-volume ratio and distinct thermodynamic properties. There is currently much interest in the solvation properties of ions in finite dimensions, such as saline atmospheric particles and nanochannels.[7−9]

The supersonic expansion + pickup principle has proved efficient for the production of mixed water clusters with dopant species and their subsequent characterization in the gas phase.[10] It has recently been applied to study alkali halides in water clusters[11,12] as well as anhydrous alkali halide clusters[12−15] with X-ray photoelectron spectroscopy (XPS). It was reported that the binding energies (BEs) of nanosolvated alkali and halide ions are insensitive to the counterions in water clusters with a few hundred water molecules,[11] similar to what has been observed in bulk solutions.[16] Notable BE discrepancies however remained, especially for the anion core levels that were attributed to calibration uncertainty in bulk level studies. In a later study, the effect of changing salt concentration was addressed with signatures of ion pairing observed in the core level spectra.[12]

A particular question lies on what size regime and how well the large cluster size limit corresponds to properties of bulk solutions.[16,17] Winter et al.[16] considered that the convergence of ionization potentials to bulk values is relatively slow due to long-range solvent polarization effects, the population of interior and surface solvation sites may differ, and structural properties of low-temperature clusters differ from bulk solutions. By performing XPS on salt-containing clusters of growing size, the sensitivity of the electronic structure to varying solvation configurations and the extent of ion−ion and ion−solvent interactions can be investigated. These questions are particularly timely now that electron spectroscopy is being increasingly applied to in situ and operando chemical analysis in wet conditions, largely enabled by liquid microjets[18] and ambient pressure setups,[19] which are available also at modern high brilliance synchrotrons.[20] In particular, surface-sensitive XPS has gained popularity in studying the liquid–vapor interface with atmospheric implications,[21−23] and the role of finite size effects should be investigated.

In this work, we report core and valence level (Cl 2p, Cl 3p, K 3p) photoelectron spectra of KCl embedded in water clusters with hundreds of water molecules. The sensitivity of

Received: February 19, 2021
Revised: April 22, 2021
Published: May 26, 2021

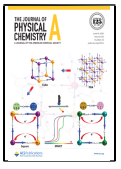

https://doi.org/10.1021/acs.jpca.1c01539
J. Phys. Chem. A 2021, 125, 4750–4759

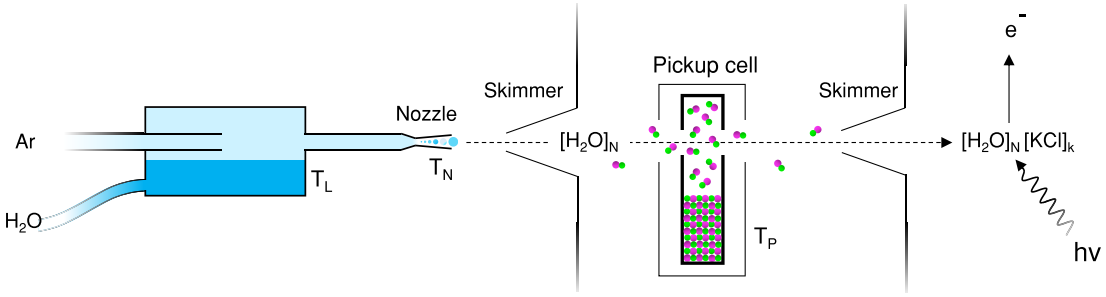

Figure 1. Schematic illustration of the experiment.

the electronic structure to cluster size and salt concentration is assessed, and the intrinsic properties of the clusters are discussed. KCl is a naturally abundant alkali halide with various applications, and its electronic structure has been broadly investigated with XPS as free molecules,[11,14,24] clusters of $[H_2O]_N[KCl]_k$[11] and $[KCl]_N$,[14] bulk KCl solutions,[16,25] and solid KCl.[24] Unique solvation properties in the nanoaqueous environment can thus be assessed by a detailed comparison of the results to these various reference systems.

EXPERIMENTAL METHODS

The experiment was carried out at the gas phase end station[26] of the newly established FinEstBeAMS beamline[27] at MAX IV synchrotron laboratory (Lund, Sweden). The clusters were generated with the new Molecular Multi Use Setup for Clusters Emission (MUSCLE), which is based on the earlier EXMEC[28] design. Figure 1 shows a schematic illustration of the experiment. Pure water clusters were generated in a continuous supersonic gas expansion and subsequently doped with KCl. Ultrapure water (18.2 MΩ·cm at 25 °C) and anhydrous potassium chloride powder of ≥99% purity (Sigma-Aldrich) were used. A conical nozzle with a minimum diameter of $d_N = 188 \pm 5$ μm, a half opening angle α of 5 ° and a ∼20 mm long expansion cone were used. The temperature of the nozzle was set to $T_N = 100 \pm 2$ °C. Two different cluster size distributions are compared to assess the size sensitivity of the spectra. With water heated to $T_L = 80$ °C, the smaller size was generated at a $P = 500 \pm 10$ mbar pure water vapor expansion pressure. The larger size was generated by using argon as a carrier gas with a total $P = 1000 \pm 100$ mbar expansion pressure. The expansion pressure was monitored using a gas-independent absolute capacitance manometer. Employing the conventional scaling laws,[29,30] the mean number of water molecules is estimated to be $\langle N\rangle_S = 160^{250}_{50}$ ($d \sim 2$ nm[31]) and $\langle N\rangle_L = 500^{1000}_{100}$ ($d \sim 3$ nm) for the smaller and larger sizes, respectively. The lower and upper indices indicate the minimum and maximum estimates of the mean size. The widths of the size distributions are expected to be $\sim\langle N\rangle$.[29] The liquid, the nozzle, and the pickup cell were Joule-heated, and the temperatures were monitored using K-type thermocouples. Beam skimmers were placed before (∼0.8 mm orifice) and after (∼3 mm orifice) the pickup cell. Details of the used pickup cell are given elsewhere.[32]

Photoelectron spectra were measured using a hemispherical deflection analyzer, Scienta R4000, aligned perpendicular to both the cluster beam and the X-ray beam. The observation angle was parallel to the light polarization axis. In all measurements, the analyzer was operated at 50 eV pass energy, and a 0.8 mm entrance slit was used. The K 3p and Cl 3p valence spectra were measured in the same scan with 100 eV photon energy and a total experimental resolution of ∼100 meV, estimated from the Gaussian full width at half-maximum (FWHM) of the Ar 3s photoelectron peak. The Cl 2p spectra were measured separately with a photon energy of 230 eV and a resolution of ∼300 meV, estimated from the Gaussian FWHM of the Ar 2p photoelectron peaks measured separately with 280 eV (lifetime broadening from ref 33). The BE scale was calibrated to the $1b_1$ level of molecular water at 12.615 eV,[34] thus finding good agreement also for the Ar 3p, 3s, and 2p lines with their literature values[33,35] (and references therein). Details of the cluster source parameters and measured statistics for all of the presented spectra are included in the Supporting Information (SI), Table S1. Peak analysis was performed using Igor Pro software from WaveMetrics with a custom-made least-squares curve-fitting package SPANCF.[36,37] Details of the peak-fitting procedures are likewise included in the Supporting Information.

RESULTS AND DISCUSSION

Pure Water Clusters. When comparing clusters to bulk solutions, it should be considered that the electronic structure and solvation dynamics are subject to the temperature and structure of the water network.[38,39] Properties of pure water clusters, without pickup, are therefore discussed first. The phase of water clusters depends on the cooling rate in the expansion, final temperature, and size.[31,40] The melting point of water clusters is lower than that of bulk water, on the order of ∼170 K for $N = 160$ and ∼210 K for $N = 500$.[31] The temperature of the clusters cannot be directly retrieved from the present data but typical estimates are well below or around these values.[40−44] Water clusters of this size range are often presumed frozen and even referred to as "ice nanoparticles".[44] The water network of small water clusters is largely amorphous (as of liquid), and partial crystallinity can occur when $N \gtrsim 90$.[40] Irregular geometries may also occur.[45]

To evaluate the similarity of the electronic structure of our pure water clusters to bulk water, we consider the vertical binding energy (VBE) of the water $1b_1$ valence level, which decreases with increasing cluster size and bridges the transition from single molecules to bulk.[30] At present, there is however no widespread consensus on the precise $1b_1$ VBE of the bulk liquid water, which remains actively discussed due to its common use as a calibration reference of liquid jet experiments.[46−54] Values have been reported at a broad energy range, from the early assignment of 11.16(4) eV by Winter et al.[46] to the recent assignment of 11.67(15) eV by Perry et al.[49] The uncertainty relates to the inherent charging of the liquid, which is often compensated with bias voltages and/or a specific electrolyte concentration.[52] This was not necessary for the present experiment, making the calibration to gas-phase

https://doi.org/10.1021/acs.jpca.1c01539
J. Phys. Chem. A 2021, 125, 4750−4759

references more straightforward. Inconsistencies in VBEs for both the solvent and solute levels between the clusters in our experiment and bulk solutions can thus reflect both finite size effects and calibration differences, and the different contributions are difficult to distinguish as such. On the other hand, the remaining uncertainty encourages one to consider how well the bulk assignments are in line with the size-dependent and eventually converging trends of gas-phase clusters.

The $1b_1$ valence spectra obtained in the present experiment are shown in Figure 2. For both water clusters and liquid jets,

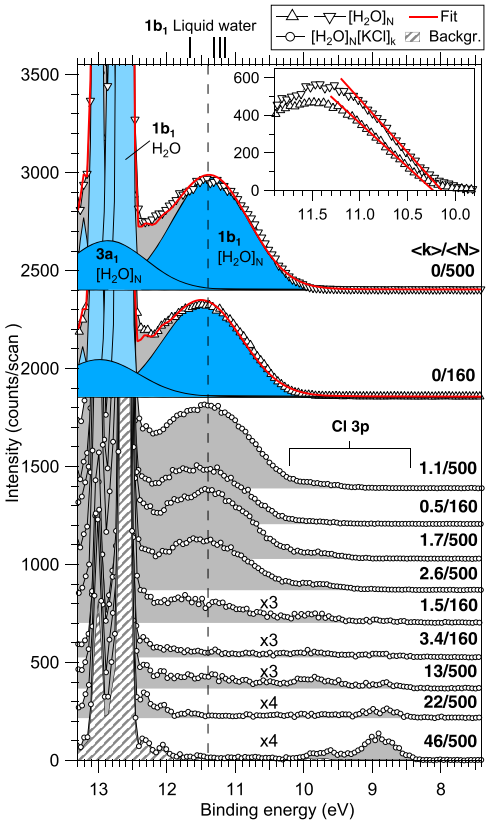

Figure 2. Photoelectron spectra in the water $1b_1$ valence region, measured with a photon energy of 100 eV. Vertical offsets have been applied for clarity. From top to bottom, the spectra are organized in order of increasing concentration, $\langle k\rangle/\langle N\rangle$, where $\langle k\rangle$ denotes the (lower limit of) mean number of picked-up molecules and $\langle N\rangle$ the mean initial cluster size (160_{50}^{250} or 500_{100}^{1000}). A background spectrum (scaled independently for better comparison) without clusters is shown for reference. VBE and ionization threshold (inset) fits are shown for the pure water cluster spectra. For comparison, VBEs of liquid water reported by others are given on top of the graph.[46−49] The dashed line at 11.4 eV is a guide to the eye.

the $1b_1$ VBE is commonly obtained from a single Gaussian fit, and the same procedure is thus adopted here. For the smaller and larger pure water clusters (without pickup), we obtain VBEs (threshold BEs) of 11.5 ± 0.1 eV (10.2 ± 0.1 eV) and 11.4 ± 0.1 eV (10.1 ± 0.1 eV), respectively. The error limits account for the experimental resolution and calibration accuracy, but lowering the VBE by 0.1 eV for the larger size is clearly resolved. The threshold energies were obtained from extrapolated line fits to the low BE side, as shown in the inset on the top right corner of Figure 2. With a similar treatment, for liquid water, a threshold BE of 9.9 eV was found by Winter et al.,[46] while 10.12(15) eV was found by Perry et al.[49] The VBEs in our experiment are among the lowest reported for water clusters (see, e.g., refs 55, 56 and references therein for values by others), and settle between the reported bulk liquid values. Based on the here still resolved VBE shift between the two sizes, and the trend of results from various other experiments compiled by Gartmann et al.,[55] we expect that the VBE of our (larger) pure water clusters is still up to a couple of hundred meV above the asymptotic bulk limit. This should be noted since comparably small differences in the solute VBEs between clusters and bulk solutions are considered below. The majority of the solute VBEs from liquid jet experiments that we compare our results with have been calibrated by setting the $1b_1$ VBE to the value of Winter et al.[46] at 11.16 eV. Kurahashi et al.[48] later suggested that the value should be refined to 11.31(4) eV after eliminating the effect of the streaming potential. As noted, the matter still remains under discussion,[52−54] but the trend of $1b_1$ VBE of water clusters[55] anyway seems to converge toward a similar energy range as the above-mentioned liquid jet values by Kurahashi et al.[48] and Winter et al.[46] The much lower temperature of the clusters may result in some discrepancy in the $1b_1$ VBE between the large cluster size limit and liquid jets. Under the assumptions that the $1b_1$ VBE decreases monotonously with increasing cluster size[55] and increasing temperature,[46] a slightly higher $1b_1$ VBE would be expected for neutral water clusters. When considering the size−energy relation of clusters probed in supersonic beams, it should be realized that the ionization probability of a cluster is proportional to the number of molecules in it, and therefore, the photoelectron spectra effectively represent a larger size distribution than the actual beam composition[55] (depending also on the probe depth for sizes when the electron mean free path becomes comparable/shorter than the dimensions of the cluster). This also applies to considering the effectively probed salt concentration for the mixed salt−water clusters, which are discussed next.

Pickup Process. Upon heating the pickup cell, signatures from KCl-doped water clusters gradually appeared in the photoelectron spectra, as seen in Figures 2 and 3. In the pickup cell, the salt evaporates mainly as neutral KCl monomers and to a lesser extent as $[KCl]_2$ dimers, which are adsorbed on the initially pure water clusters. Distinct from the earlier experiments,[11,12] a double skimmer configuration and a longer cluster flight path were used, which allowed extraction of the mixed cluster spectra (particularly the outermost valence) with the less overlapping signal from free KCl and $[KCl]_2$ effusing from the pickup oven.[11,12] The mean number of picked-up molecules $\langle k\rangle$ follows a Poisson distribution[57] and scales with the density $\rho \sim p(T)/T_P$ of KCl, where $p(T)$ is the vapor pressure[58] and T_P is the temperature of KCl. More specifically, the given values represent the estimated lower limit of $\langle k\rangle$ and, accordingly, the true values should be somewhat higher. The estimation procedure of $\langle k\rangle$ is described in the Supporting Information.

The roles of low temperature, finite size, and limited relaxation time before the X-ray probe are to be considered when discussing the accommodation process of the salt to the water cluster. The initial cluster size is well above the requirements to favor charge separation with low concentrations.[6,59−61] In bulk conditions, the first hydration shell of both K^+ and Cl^- ions contains ∼6 water molecules and the ion−water distance is ∼0.3 nm to the first hydration shell and ∼0.5 nm to the second.[62] The cluster size is thus sufficiently

https://doi.org/10.1021/acs.jpca.1c01539
J. Phys. Chem. A 2021, 125, 4750−4759

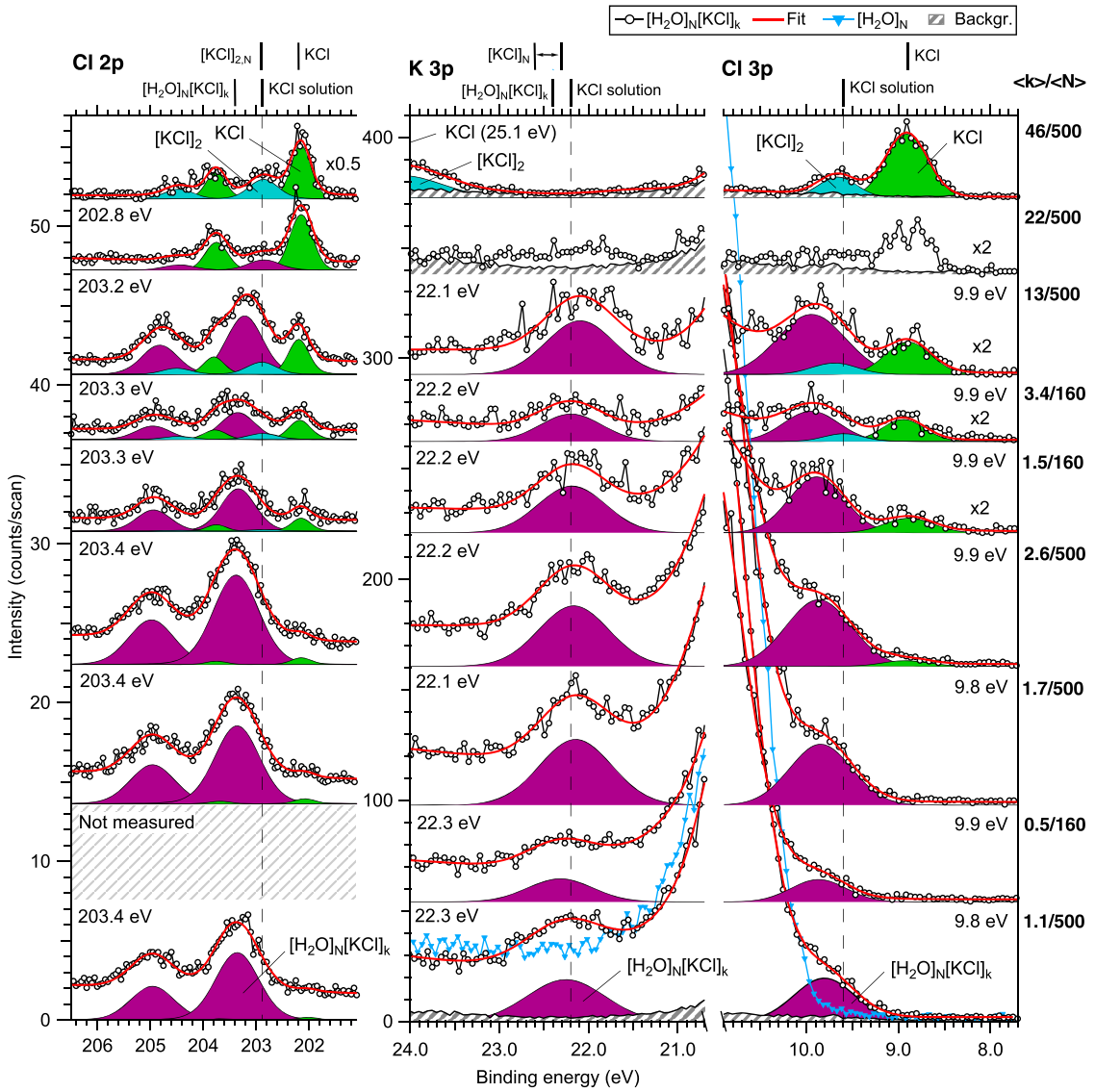

Figure 3. Photoelectron spectra in the Cl 2p (left), K 3p (center), and Cl 3p (right) regions. From bottom to top, the spectra are organized in order of increasing concentration, $\langle k\rangle/\langle N\rangle$, where $\langle k\rangle$ denotes the (lower limit of) mean number of picked-up molecules and $\langle N\rangle$ is the mean initial cluster size (160^{250}_{50} or 500^{1000}_{100}). Vertical offsets have been applied for clarity. The Cl 2p spectra were measured with a photon energy of 230 eV, while the K 3p and Cl 3p spectra were measured with 100 eV. Background (scaled independently) and pure water cluster spectra are also shown for comparison. VBEs of the fitted mixed cluster peaks are designated in the corner of each spectrum. For comparison, experimental VBEs from other reports are given on top of the graph for KCl,[14] $[KCl]_N$,[1414] $[H_2O]_N[KCl]_M$,[11] and KCl solutions.[16,25]

large to form multiple hydration layers around the ions, at least when the number of available water molecules is concerned. Localization of the ions to the cluster interior/surface is of interest. Recent studies suggest that in both clusters and bulk solutions, (heavy) halide anions are favorably positioned near the liquid−vapor interface, while alkali cations are more likely found below the immediate surface.[21,23,63−66] The population of surface/interior sites likely differs between clusters and bulk solutions,[16] considering the large surface-to-volume ratio, surface curvature,[67] and low-temperature effects. Molecular dynamics (MD) simulations by Zhao et al.,[64] Sun et al.,[68] and Liu et al.[69] on ion-containing water clusters suggest that Cl^- ions have a tendency to locate near to the cluster surface region but do not necessarily lie explicitly at the surface. In our experiment, one should however specifically consider the adsorption and solvation of an alkali halide molecule into a cold water cluster, and we are unaware of any simulations performed on directly analogous conditions. Charge separation is likely, despite the low internal temperature of the water clusters, as our (and earlier[11]) results also suggest. Alkali halides are known to readily dissolve also when adsorbed on ice films.[70−73] However, if the cluster is frozen, one can argue whether a rigid water network will reduce the mobility of the salt and even prevent submergence of the ions.[73] In similar experiments, various atomic and molecular species (and electrons) adsorbed on water clusters have been observed to remain on the surface.[42,74−76]

With alkali halides, a significant amount of energy is however brought into the system in the pickup process. We estimate that, in a single pickup event of KCl, the collision energy (internal energy of KCl + kinetic energy of the collision) is on the order of ∼500 meV, and that a further ∼2300 meV is released from charge separation (see the Supporting Information for calculation). Assuming that these energies

https://doi.org/10.1021/acs.jpca.1c01539
J. Phys. Chem. A 2021, 125, 4750−4759

are fully transferred to the internal energy of the cluster, the cluster temperature is raised by several tens of Kelvins, depending on the cluster size (rough estimates for the temperature change are provided in the Supporting Information). This means that if the water cluster is initially frozen, melting is potentially induced, especially when multiple pickup events occur. This may induce substantial reorganization of the cluster, e.g., migration of ions to the interior in the sub-nanosecond timescale[68]. Due to the simultaneously increasing rate of evaporative cooling, such high-temperature states would however be much shorter-lived than the approximately half a millisecond flight time of the clusters between pickup and the X-ray probe, given a cluster speed of ∼1000 m/s. Considering the evaporative cooling simulations on pure and ion-containing water clusters by Caleman and van der Spoel,[77,78] we do not expect to be probing clusters at temperatures ≫200 K (depending also on the salt content). Thus, similar to the pure water clusters, the internal temperature of the mixed salt−water clusters should also be inevitably lower than accessible, e.g., in liquid jets.[16] On the other hand, such low temperatures are typical for atmospheric particles, especially at high altitudes.

With an increasing number of picked-up molecules, evaporative cooling reduces the cluster size and therefore also effectively increases the concentration. The combined collision + solvation energies correspond to the binding enthalpy of ∼6 water molecules.[79] Changes in the cluster size and concentration distribution are also subject to the fact that the pickup probability and diffusion losses (transverse velocity gain in pickup events) depend on the cluster size. With an increasing pickup temperature, the cluster intensity was observed to decrease and eventually vanish completely (Figure 2), which is attributed to the evaporation and diffusion effects. As this intensity decrease thus correlates with the amount of pickup, we have taken advantage of it in estimating $\langle k \rangle$, as described in the Supporting Information.

Mixed KCl−Water Clusters. The acquired Cl 2p, K 3p, and Cl 3p regions are shown in Figure 3, measured in the T_P = 480−580 °C temperature range. The spectra on the right-side column are the same as shown in Figure 2, but here the Cl 3p region is magnified and shown with the peak fits. In the majority of the fits, the VBE of the Cl 3p level is found at ∼9.9 ± 0.1 eV, being ∼1 eV higher than the free KCl monomer at 8.9 ± 0.1 eV. We are unaware of other reported experimental Cl 3p VBEs in water clusters of this size regime. Markovich et al.[1] have measured the VBE in the range 3.61−6.88 eV for smaller anionic $Cl^-[H_2O]_{0-7}$ clusters. With few to few tens of water molecules in the cluster, the binding energies are highly sensitive to the precise number of water molecules and ions in the cluster, as well as to the cluster isomer and charge state.[1,5,6,12,63,80,81] With hundreds of water molecules in the present experiment, this sensitivity appears to be notably suppressed. However, as it was already stated that the $1b_1$ VBE of the solvent has not explicitly converged to the asymptotic limit, there is reason to expect a slight deviation from bulk values also for the solute VBEs. Since in small clusters, the Cl 3p VBE gradually increases with an increasing number of water molecules,[1,81] one might expect for the present results to settle below the bulk solution value. In contrast, in all spectra, the VBEs are higher than the 9.5[48]−9.6 eV,[16,25,38,82] consistently reported from liquid jets. The ionization threshold is correspondingly higher, being 9.1 ± 0.1 eV at the lowest, while 8.7 eV has been reported from liquid jet solutions.[16] The VBE of the Cl 3p level has gained considerable theoretical interest in recent years.[83−87] Very comparable energies to our result were recently reported e.g., by Bouchafra et al.[85] on Cl^- surrounded by 50 water molecules. Olleta et al.[81] have calculated 8.51−9.90 eV for $KCl(H_2O)_{0-6}$ (some of their equilibrium structures are depicted in the abstract figure).

Photoelectron spectra of the anion core level, Cl 2p, are shown in the left-hand column of Figure 3. The spin−orbit splitting is ∼1.6 eV and, for convenience, we shall refer to VBEs of the $2p_{3/2}$ component. Previously, Partanen et al.[11] found 203.4 ± 0.2 eV for NaCl and KCl in water clusters with $\langle N \rangle$ ∼ 150−400, but the effect of concentration was not investigated (the number of picked-up molecules was estimated to be <10). In our spectra, the VBEs range from 203.2 ± 0.1 to 203.4 ± 0.1 eV. The best agreement with that of Partanen et al.[11] is found with low salt concentrations, as expected. Similar to the Cl 3p valence level, the Cl 2p VBEs are ∼1 eV higher than that of a free KCl molecule at 202.2 ± 0.1 eV, and also higher than the 202.89 eV microjet value reported by Pokapanich et al.[25] for a 2 mol/kg (∼14 water molecules per ion) KCl solution.

For the cation, the K 3p region was acquired in the same scan range with the valence spectra, shown in the center column of Figure 3. Broader views of these spectra are included in the Supporting Information. The K 3p VBE in clusters is ∼3 eV lower than in the free KCl monomer, in contrast to the anion levels that were found in clusters at higher VBEs than the monomer. The opposite directions and magnitudes of the VBE shifts relate to the increasing and decreasing strengths of electrostatic interaction with the solvent in going from the initial state to the final state, as removal of an electron changes the charge state from +1 to +2 for a cation and from −1 to 0 for an anion.[11,13,82] Previously, a K 3p VBE of 22.4 ± 0.1 eV was reported by Partanen et al.[11] for KCl, KBr, and KI in water clusters. In our spectra, the fitted VBEs range from 22.1 ± 0.1 to 22.3 ± 0.1 eV. As for Cl 2p, the best agreement is found with the result of Partanen et al.[11] in the lowest concentrations for K 3p as well. In liquid jets, a counterion-independent K 3p VBE of 22.2 eV has been reported,[16,25,82] which is within the error bars of our spectra.

As such, better agreement in VBEs is found with liquid jets for the cation than for the anion, but as already noted the direct comparison of VBEs between clusters and bulk solutions is subject to a potential calibration offset. However, it seems that this can only partly explain the discrepancies, as agreement cannot be found for all three levels simultaneously by simply shifting the energy scale in any of our spectra. Most of the referred liquid jet results were calibrated with the $1b_1$ VBE set at 11.16 eV, and if we applied this same calibration procedure the agreement would improve for the anion levels but worsen for the cation.

Structural Properties. As discussed above, the population of solvation sites likely differs between clusters and bulk solutions, although calculations do suggest that VBE shifts between surface/interior solvated ions should be rather subtle.[1,63,86,88,89] We are unaware of any liquid jet studies where VBE differences between surface/interior sites would have been resolved, e.g., by depth profiling, whereas some studies on saturated solutions on substrates have reported large splitting of the anion core levels (the cation spectra showed only a single component).[65,66,90] Various possible origins for this splitting were discussed by Tissot et al.[66] For NaCl and RbCl solutions, the Cl 2p surface component was found ∼2 eV

https://doi.org/10.1021/acs.jpca.1c01539
J. Phys. Chem. A 2021, 125, 4750−4759

higher than the interior component,[66] which is much larger than the here observed concentration-dependent shifts or VBE discrepancies to liquid jets, suggesting that we are not probing similar states.

Despite the relatively high resolution in the present experiment, no clear multipeak structures are resolved, which could allow a quantitative analysis of the population of qualitatively different chemical states such as surface/interior localized ions or solvent separated/shared/contact ion pairs (a clear two-peak structure was however observed previously for the Rb 3d core level[12]). This is in line with liquid jet observations,[16] and does not, however, necessarily exclude the presence of these different structures in the clusters as a large number of variable solvent configurations may spread in energy with significant overlap so that they are indistinguishable. We emphasize that the spectra represent statistics from a broad range of equilibrium cluster structures and sizes, where the degree of disorder (which depends also on temperature) is reflected in the broad peak widths.[4,16,91,92] The peak widths in clusters are similar to or slightly narrower than those in liquid jets for Cl 2p ∼0.7 to 1.0 eV (1 eV for the bulk solution[25]) and for K 3p ∼0.8 to 1.0 eV (1.4 ± 0.2 eV[16,82]). The same was found also for Br 3d in the RbBr experiment[12] with widths between 0.55 and 0.80 eV (1.1/1.2 ± 0.10 eV[16]). For Cl 3p, we find ∼0.7 to 0.9 eV, while two rather different values have been reported from bulk solutions (0.6 ± 0.20[16] and 0.9 ± 0.30[48]). If one assumes that, in clusters and bulk solutions, similar local (within the nearest hydration shells) solute−solvent structural moieties are probed, the differences in BEs and FWHM can be considered to reflect on the role of long-range electrostatic effects and the lower temperature of the clusters. It is however clear that the overall cluster structures can be different from perfect "snapshots" of bulk solutions due to their lower temperature, high surface area, and the fact that they are not confined in the solution, which allows additional freedom for the structural organization. Evidently, the cluster structures depend on the solvation dynamics during the pickup process, as discussed above.

Concentration Effects. In an earlier experiment with another alkali halide, RbBr in water clusters, VBE shifts were observed with increasing pickup in the probed Rb 3d and Br 3d core levels, which were attributed to increasing ion pairing.[12] The anion core level (Br 3d) was observed to shift to lower VBE and simultaneously the peak width was narrowed. Here, with KCl, the Cl 2p level behaves similarly. A particular −0.15 eV jump is observed in the $\langle k \rangle \sim 13$ spectrum, in which the water content in the clusters relative to salt is significantly lower as seen in Figure 2. The higher concentration spectra with $\langle k \rangle \sim 22$ and 46 are found at still lower VBEs, but the broad peaks likely contain a significant amount of $[KCl]_2$ as well, and the cluster contribution (and VBE) cannot be reliably assessed. The signal from water in these clusters is (almost) negligible. In the highest temperature spectra ($\langle k \rangle \sim 46$), the observed features in all three levels seem to originate from free KCl and $[KCl]_2$ only. It can be considered that when concentration increases, the Cl 2p VBE shifts slightly closer to that reported for both anhydrous ($[KCl]_N$[11,14]) and hydrous (liquid KCl solution[25]) multi-ionic systems, which coincide at ∼202.9 eV. Note that the number of picked-up molecules is not, in principle, limited by solubility. For the cation core level Rb 3d (VBE ∼ 115 eV), a second feature at ∼1 eV higher VBE was observed with increasing concentration of RbBr,[12] where the lower VBE feature was attributed to fully solvated ions and the higher VBE feature to solvent shared and contact ion pairs. Here, we do not resolve similar splitting for the K 3p level, which may reflect that K 3p is a valence orbital and does not express comparably large VBE shifts. Some variation is found in the average VBE and FWHM of K 3p over the probed concentration range, but not in an entirely monotonous manner. We refrain from fitting the K 3p and Cl 3p spectra with $\langle k \rangle \sim 22$ due to low statistics, but we note that in both levels signal is still observed at energies comparable to the lower temperature spectra, albeit that there is an almost negligible signal from water in the clusters.

The effect of concentration has been addressed also for bulk solutions in liquid jets but negligible or only very subtle VBE shifts have been reported.[16,51,82,93] We are unaware of any reported changes in Cl 2p, K 3p, and Cl 3p VBEs with changing alkali halide concentration in liquid jets, besides that two rather different VBEs have been observed for Cl 2p in separate experiments (202.89 eV for 2 mol/kg KCl[25] and 202.1 eV for 3 mol/kg LiCl[91]), which Pokapanich et al. considered to possibly indicate the dependence of the VBE on counter ion or concentration. Recently, Pohl et al.[51] studied NaI solutions over a broad concentration range of 0.5−8.0 M (∼56 to 3 water molecules per ion). They reported that the VBE of the I 4d level decreased up to 0.15 ± 0.06 eV and the 5p valence level up to 0.11 ± 0.06 eV, while no shift was observed for the Na 2p level of the cation (referencing the energies to the $1b_1$ level of the solution). They speculated that at higher concentrations, charge donation from the anion to the solvent is affected as the water network becomes increasingly disrupted. The slightly decreasing VBE of the anion core level (I 4d) is qualitatively similar to that found here for Cl 2p and previously for Br 3d[12] in water clusters. There are however also cluster-specific effects that must be considered in assessing the origin of the observed concentration dependence of VBEs and FWHMs in clusters. As discussed above, besides the increasing salt concentration, the cluster size and temperature are also varied with an increasing number of adsorbed salt molecules. In this sense, the observations are not entirely comparable to the bulk solution case.

Since the clusters are generated essentially by in-vacuum condensation of neutral water and salt molecules, they can be considered to be electrically neutral and contain an equal number of cations and anions. This assumption may break down if charge evaporation from the pickup oven or from the clusters occurs during the pickup process, which could also lead to VBE shifts, although we expect this effect to be minor at least when the number of picked-up molecules is small. We emphasize that the results are however not subject to structural changes subsequent to photoionization due to the instantaneous nature of the ionization process and that no permanent radiation damage can play a role due to the constantly renewable particle beam.

Finally, the effect of the solute on the solvent electronic levels is also of interest, particularly to the VBE of $1b_1$. In Figure 2, the cluster $1b_1$ peak is seen to decrease in intensity with increasing salt content, but also its shape is modified and weighted to higher VBEs. Similar behavior was observed also in the RbBr experiment.[12] This implies that shifting of the solvent VBEs may occur due to the effect of the ions. We note that this would contrast the conclusion of Pohl et al.[51] that, in a bulk solution, the electrolyte (NaI) has a minimal effect on the $1b_1$ VBE, justifying its use as a calibration reference.

https://doi.org/10.1021/acs.jpca.1c01539
J. Phys. Chem. A 2021, 125, 4750−4759

However, as discussed for the solute spectra, cluster-specific effects can play a role here as well. Both pure and mixed clusters are probed simultaneously with varying relative intensities, which are inseparable from the solvent spectra. Besides the salt concentration, size distributions of the pure and mixed cluster fractions are modified since the pickup probability as well as evaporation and diffusion effects depend on the cluster size and the number of picked-up molecules (see also, e.g., ref 94), which can also be responsible for the observed BE shift. Further investigation would be needed for clarification.

CONCLUSIONS

Nanosolvation of KCl in gas-phase water clusters has been investigated with core and valence level photoelectron spectroscopy. The results indicate that with hydration states of a few hundred water molecules, the electronic structure of the solute no longer shows high sensitivity to cluster size, as reflected in the VBEs of the probed Cl 2p, Cl 3p, and K 3p levels. Yet, the observed VBEs and FWHM do not fully agree with those observed near the liquid−vapor interface of bulk solutions. In particular, the VBE of the Cl 3p valence level at 9.9 ± 0.1 eV, as well as the Cl 2p core level, do not settle between that of the free KCl monomer (8.9 ± 0.1 eV) and liquid jet solutions (9.6 ± 0.07 eV[16]). Further investigations are needed to clarify the role of unique structural properties, low-temperature effects, calibration differences, and the finite extent of long-range electrostatic ion−ion and ion−solvent interactions in the nanoaqueous environment. In future experiments, we expect that the structural properties of the clusters will be further elucidated by the combination of electron spectroscopy with other techniques such as X-ray absorption spectroscopy,[95,96] mass spectroscopy,[44,55,75] and multiparticle coincidence experiments.[97] The reported experimental VBEs offer relevant benchmarks for theoretical works.

ASSOCIATED CONTENT

Supporting Information

The Supporting Information is available free of charge at https://pubs.acs.org/doi/10.1021/acs.jpca.1c01539.

Details of the clustering conditions and data collection; peak fitting procedures; pickup estimation; estimation of collision and solvation energies; and broader views of the photoelectron spectra (PDF)

AUTHOR INFORMATION

Corresponding Author

Eetu Pelimanni − *Nano and Molecular Systems Research Unit, Faculty of Science, University of Oulu, FI-90014 Oulu, Finland;* orcid.org/0000-0002-4550-6430; Email: eetu.pelimanni@oulu.fi

Authors

Lauri Hautala − *Nano and Molecular Systems Research Unit, Faculty of Science, University of Oulu, FI-90014 Oulu, Finland*

Andreas Hans − *Nano and Molecular Systems Research Unit, Faculty of Science, University of Oulu, FI-90014 Oulu, Finland; Universität Kassel, Institut für Physik und CINSaT, 34132 Kassel, Germany;* orcid.org/0000-0002-4176-4766

Antti Kivimäki − *Nano and Molecular Systems Research Unit, Faculty of Science, University of Oulu, FI-90014 Oulu, Finland; MAX IV Laboratory, Lund University, SE-22100 Lund, Sweden;* orcid.org/0000-0003-0753-8164

Mati Kook − *Institute of Physics, University of Tartu, EE-50411 Tartu, Estonia*

Catmarna Küstner-Wetekam − *Universität Kassel, Institut für Physik und CINSaT, 34132 Kassel, Germany*

Lutz Marder − *Universität Kassel, Institut für Physik und CINSaT, 34132 Kassel, Germany*

Minna Patanen − *Nano and Molecular Systems Research Unit, Faculty of Science, University of Oulu, FI-90014 Oulu, Finland;* orcid.org/0000-0002-2970-7494

Marko Huttula − *Nano and Molecular Systems Research Unit, Faculty of Science, University of Oulu, FI-90014 Oulu, Finland*

Complete contact information is available at: https://pubs.acs.org/10.1021/acs.jpca.1c01539

Notes

The authors declare no competing financial interest.

ACKNOWLEDGMENTS

The authors gratefully acknowledge funding from the Academy of Finland (project grants Nos. 296338, 306984, 328467, and InStreams profiling grant No. 326291). E.P. acknowledges funding from the Finnish Cultural Foundation, North Ostrobothnia Regional fund (60192221). A.H., C.K.-W. and L.M. acknowledge funding by the Deutsche Forschungsgemeinschaft (DFG) (Project No. 328961117—SFB 1319 ELCH). M.K. acknowledges support by the Graduate School of Functional Materials and Technologies, University of Tartu (2014-2020.4.01.16-0027), and Centres of Excellence project "Advanced materials and high-technology devices for sustainable energetics, sensorics and nanoelectronics" TK141 (2014-2020.4.01.15-0011). The authors are thankful to MAX IV Laboratory for time on Beamline FinEstBeAMS under Proposal 20190638. Research conducted at MAX IV, a Swedish national user facility, is supported by the Swedish Research council under contract 2018-07152, the Swedish Governmental Agency for Innovation Systems under contract 2018-04969, and Formas under contract 2019-02496. Dr. Mikko-Heikki Mikkelä, Paavo Turunen, and Dr. Kirill Chernenko are acknowledged for their help in the construction of the experimental setup.

REFERENCES

(1) Markovich, G.; Pollack, S.; Giniger, R.; Cheshnovsky, O. Photoelectron Spectroscopy of Cl-, Br-, and I- Solvated in Water Clusters. *J. Chem. Phys.* **1994**, *101*, 9344−9353.

(2) Castleman, A.; Bowen, K. Clusters: Structure, Energetics, and Dynamics of Intermediate States of Matter. *J. Phys. Chem.* **1996**, *100*, 12911−12944.

(3) Dedonder-Lardeux, C.; Grégoire, G.; Jouvet, C.; Martrenchard, S.; Solgadi, D. Charge Separation in Molecular Clusters: Dissolution of a Salt in a Salt-(Solvent)n Cluster. *Chem. Rev.* **2000**, *100*, 4023−4038.

(4) Bradforth, S. E.; Jungwirth, P. Excited States of Iodide Anions in Water: A Comparison of the Electronic Structure in Clusters and in Bulk Solution. *J. Phys. Chem. A* **2002**, *106*, 1286−1298.

(5) Li, R.-Z.; Liu, C.-W.; Gao, Y. Q.; Jiang, H.; Xu, H.-G.; Zheng, W.-J. Microsolvation of LiI and CsI in Water: Anion Photoelectron Spectroscopy and ab initio Calculations. *J. Am. Chem. Soc.* **2013**, *135*, 5190−5199.

(6) Hou, G.-L.; Liu, C.-W.; Li, R.-Z.; Xu, H.-G.; Gao, Y. Q.; Zheng, W.-J. Emergence of Solvent-Separated Na.−Cl− Ion Pair in Salt Water: Photoelectron Spectroscopy and Theoretical Calculations. *J. Phys. Chem. Lett.* **2017**, *8*, 13−20.
(7) Antonsson, E.; Patanen, M.; Nicolas, C.; Neville, J. J.; Benkoula, S.; Goel, A.; Miron, C. Complete Bromide Surface Segregation in Mixed NaCl/NaBr Aerosols Grown from Droplets. *Phys. Rev. X* **2015**, *5*, No. 011025.
(8) Li, H.; Francisco, J. S.; Zeng, X. C. Unraveling the Mechanism of Selective Ion Transport in Hydrophobic Subnanometer Channels. *Proc. Natl. Acad. Sci. U.S.A.* **2015**, *112*, 10851−10856.
(9) Bzdek, B. R.; Reid, J. P.; Malila, J.; Prisle, N. L. The Surface Tension of Surfactant-Containing, Finite Volume Droplets. *Proc. Natl. Acad. Sci. U.S.A.* **2020**, *117*, 8335−8343.
(10) Fárník, M.; Fedor, J.; Kocisek, J.; Lengyel, J.; Pluharova, E.; Poterya, V.; Pysanenko, A. Pickup and Reactions of Molecules on Clusters Relevant for Atmospheric and Interstellar Processes. *Phys. Chem. Chem. Phys.* **2021**, *23*, 3195−3213.
(11) Partanen, L.; Mikkelä, M.-H.; Huttula, M.; Tchaplyguine, M.; Zhang, C.; Andersson, T.; Björneholm, O. Solvation at Nanoscale: Alkali-Halides in Water Clusters. *J. Chem. Phys.* **2013**, *138*, No. 044301.
(12) Hautala, L.; Jänkälä, K.; Mikkelä, M.-H.; Turunen, P.; Prisle, N. L.; Patanen, M.; Tchaplyguine, M.; Huttula, M. Probing RbBr Solvation in Freestanding sub-2 nm Water Clusters. *Phys. Chem. Chem. Phys.* **2017**, *19*, 25158−25167.
(13) Zhang, C.; Andersson, T.; Svensson, S.; Björneholm, O.; Huttula, M.; Mikkelä, M.-H.; Tchaplyguine, M.; Öhrwall, G. Ionic Bonding in Free Nanoscale NaCl Clusters as Seen by Photoelectron Spectroscopy. *J. Chem. Phys.* **2011**, *134*, No. 124507.
(14) Zhang, C.; Andersson, T.; Svensson, S.; Björneholm, O.; Huttula, M.; Mikkelä, M.-H.; Anin, D.; Tchaplyguine, M.; Öhrwall, G. Holding onto Electrons in Alkali Metal Halide Clusters: Decreasing Polarizability with Increasing Coordination. *J. Phys. Chem. A* **2012**, *116*, 12104−12111.
(15) Hautala, L.; Jänkälä, K.; Mikkelä, M.-H.; Tchaplyguine, M.; Huttula, M. Surface Site Coordination Dependent Responses Resolved in Free Clusters: Applications for Neutral sub-nanometer Cluster Studies. *Phys. Chem. Chem. Phys.* **2015**, *17*, 7012−7022.
(16) Winter, B.; Weber, R.; Hertel, I. V.; Faubel, M.; Jungwirth, P.; Brown, E. C.; Bradforth, S. E. Electron Binding Energies of Aqueous Alkali and Halide Ions: EUV Photoelectron Spectroscopy of Liquid Solutions and Combined Ab Initio and Molecular Dynamics Calculations. *J. Am. Chem. Soc.* **2005**, *127*, 7203−7214.
(17) Gupta, P. K.; Schienbein, P.; Daru, J.; Marx, D. Terahertz Spectra of Microsolvated Ions: do They Reveal Bulk Solvation Properties. *J. Phys. Chem. Lett.* **2019**, *10*, 393−398.
(18) Seidel, R.; Winter, B.; Bradforth, S. E. Valence Electronic Structure of Aqueous Solutions: Insights from Photoelectron Spectroscopy. *Annu. Rev. Phys. Chem.* **2016**, *67*, 283−305.
(19) Schnadt, J.; Knudsen, J.; Johansson, N. Present and New Frontiers in Materials Research by Ambient Pressure X-ray Photoelectron Spectroscopy. *J. Phys.: Condens. Matter* **2020**, *32*, No. 413003.
(20) Urpelainen, S.; Såthe, C.; Grizolli, W.; Agåker, M.; Head, A. R.; Andersson, M.; Huang, S.-W.; Jensen, B. N.; Wallén, E.; Tarawneh, H.; et al. The SPECIES Beamline at the MAX IV Laboratory: A facility for Soft X-ray RIXS and APXPS. *J. Synchrotron Radiat.* **2017**, *24*, 344−353.
(21) Ghosal, S.; Hemminger, J. C.; Bluhm, H.; Mun, B. S.; Hebenstreit, E. L. D.; Ketteler, G.; Ogletree, D. F.; Requejo, F. G.; Salmeron, M. Electron Spectroscopy of Aqueous Solution Interfaces Reveals Surface Enhancement of Halides. *Science* **2005**, *307*, 563−566.
(22) Werner, J.; Julin, J.; Dalirian, M.; Prisle, N. L.; Öhrwall, G.; Persson, I.; Björneholm, O.; Riipinen, I. Succinic Acid in Aqueous Solution: Connecting Microscopic Surface Composition and Macroscopic Surface Tension. *Phys. Chem. Chem. Phys.* **2014**, *16*, 21486−21495.
(23) Gladich, I.; Chen, S.; Vazdar, M.; Boucly, A.; Yang, H.; Ammann, M.; Artiglia, L. Surface Propensity of Aqueous Atmospheric Bromine at the Liquid−Gas Interface. *J. Phys. Chem. Lett.* **2020**, *11*, 3422−3429.
(24) Patanen, M.; Bancroft, G. M.; Aksela, S.; Aksela, H. Direct experimental determination of the K 2p and Cl 2p core-level binding energy shifts between molecular and solid KCl: Line broadening effects. *Phys. Rev. B* **2012**, *85*, No. 125419.
(25) Pokapanich, W.; Bergersen, H.; Bradeanu, I. L.; Marinho, R. R. T.; Lindblad, A.; Legendre, S.; Rosso, A.; Svensson, S.; O., B.; Tchaplyguine, M.; et al. Auger Electron Spectroscopy as a Probe of the Solution of Aqueous Ions. *J. Am. Chem. Soc.* **2009**, *131*, 7264−7271.
(26) Kooser, K.; Kivimäki, A.; Turunen, P.; Pärna, R.; Reisberg, L.; Kirm, M.; Valden, M.; Huttula, M.; Kukk, E. Gas-phase Endstation of Electron, Ion and Coincidence Spectroscopies for Diluted Samples at the FinEstBeAMS Beamline of the MAXIV 1.5 GeV Storage Ring. *J. Synchrotron Radiat.* **2020**, *27*, 1080−1091.
(27) Pärna, R.; Sankari, R.; Kukk, E.; Nõmmiste, E.; Valden, M.; Lastusaari, M.; Kooser, K.; Kokko, K.; Hirsimäki, M.; Urpelainen, S.; et al. FinEstBeaMS − A Wide-range Finnish-Estonian Beamline for Materials Science at the 1.5 GeV Storage Ring at the MAX IV Laboratory. *Nucl. Instrum. Methods Phys. Res., Sect. A* **2017**, *859*, 83−89.
(28) Huttula, M.; Mikkelä, M.-H.; Tchaplyguine, M.; Björneholm, O. Size-varied Photoelectron Spectroscopy of Metal Clusters Using the Exchange Metal Cluster Source. *J. Electron Spectrosc. Relat. Phenom.* **2010**, *181*, 145−149.
(29) Bobbert, C.; Schütte, S.; Steinbach, C.; Buck, U. Fragmentation and Reliable Size Distributions of Large Ammonia and Water Clusters. *Eur. Phys. J. D* **2002**, *19*, 183−192.
(30) Barth, S.; Ončák, M.; Ulrich, V.; Mucke, M.; Lischke, T.; Slavíček, P.; Hergenhahn, U. Valence Ionization of Water Clusters: From Isolated Molecules to Bulk. *J. Phys. Chem. A* **2009**, *113*, 13519−13527.
(31) Johnston, J. C.; Molinero, V. Crystallization, Melting, and Structure of Water Nanoparticles at Atmospherically Relevant Temperatures. *J. Am. Chem. Soc.* **2012**, *134*, 6650−6659.
(32) Hautala, L. Synchrotron Radiation Based Characterization of Structural Evolution of Alkali Halide Clusters. Ph.D. Thesis; University of Oulu, 2017.
(33) Carroll, T. X.; Bozek, J. D.; Kukk, E.; Myrseth, V.; Saethre, L. J.; Thomas, T. D. Line Shape and Lifetime in Argon 2p Electron Spectroscopy. *J. Electron Spectrosc. Relat. Phenom.* **2001**, *120*, 67−76.
(34) Karlsson, L.; Mattsson, L.; Jadrny, R.; Albridge, R. G.; Pinchas, S.; Bergmark, T.; Siegbahn, K. Isotopic and Vibronic Coupling Effects in the Valence Electron Spectra of $H_2{}^{16}O$, $H_2{}^{18}O$, and $D_2{}^{16}O$. *J. Chem. Phys.* **1975**, *62*, 4745−4752.
(35) Kramida, A.; Ralchenko, Y.; Reader, J. NIST ASD Team, *NIST Atomic Spectra Database*, version 5.8; National Institute of Standards and Technology: Gaithersburg, MD, https://physics.nist.gov/asd (November 23, 2020).
(36) Kukk, E.; Snell, G.; Bozek, J. D.; Cheng, W.-T.; Berrah, N. Vibrational Structure and Partial Rates of Resonant Auger Decay of the N1s $\rightarrow 2\pi$ Core Excitations in Nitric Oxide. *Phys. Rev. A* **2001**, *63*, No. 062702.
(37) Kukk, E.; Ueda, K.; Hergenhahn, U.; Liu, X.-J.; Prümper, G.; Yoshida, H.; Tamenori, Y.; Makochekanwa, C.; Tanaka, T.; Kitajima, M.; et al. Violation of the Franck-Condon Principle due to Recoil Effects in High Energy Molecular Core-Level Photoionization. *Phys. Rev. Lett.* **2005**, *95*, No. 133001.
(38) Winter, B.; Faubel, M.; Hertel, I. V.; Pettenkofer, C.; Bradforth, S. E.; Jagoda-Cwiklik, B.; Cwiklik, L.; Jungwirth, P. Electron Binding Energies of Hydrated H3O. and OH-: Photoelectron Spectroscopy of Aqueous Acid and Base Solutions Combined with Electronic Structure Calculations. *J. Am. Chem. Soc.* **2006**, *128*, 3864−3865.
(39) Nordlund, D.; Odelius, M.; Bluhm, H.; Ogasawara, H.; Pettersson, L.; Nilsson, A. Electronic Structure Effects in Liquid

https://doi.org/10.1021/acs.jpca.1c01539
J. Phys. Chem. A 2021, 125, 4750−4759

Water Studied by Photoelectron Spectroscopy and Density Functional Theory. *Chem. Phys. Lett.* **2008**, *460*, 86−92.
(40) Moberg, D. R.; Becker, D.; Dierking, C. W.; Zurheide, F.; Bandow, B.; Buck, U.; Hudait, A.; Molinero, V.; Paesani, F.; Zeuch, T. The End of Ice I. *Proc. Natl. Acad. Sci. U.S.A.* **2019**, *116*, 24413−24419.
(41) Torchet, G.; Schwartz, P.; Farges, J.; de Feraudy, M. F.; Raoult, B. Structure of Solid Water Clusters Formed in a Free Jet Expansion. *J. Chem. Phys.* **1983**, *79*, 6196−6202.
(42) Pradzynski, C. C.; Forck, R. M.; Zeuch, T.; Slavíček, P.; Buck, U. A Fully Size-Resolved Perspective on the Crystallization of Water Clusters. *Science* **2012**, *337*, 1529−1532.
(43) Buck, U.; Pradzynski, C. C.; Zeuch, T.; Dieterich, J. M.; Hartke, B. A Size Resolved Investigation of Large Water Clusters. *Phys. Chem. Chem. Phys.* **2014**, *16*, 6859−6871.
(44) Fárník, M.; Lengyel, J. Mass Spectrometry of Aerosol Particle Analogues in Molecular Beam Experiments. *Mass Spectrom. Rev.* **2018**, *37*, 630−651.
(45) Lengyel, J.; Pysanenko, A.; Poterya, V.; Slavíček, P.; Fárník, M.; Kočišek, J.; Fedor, J. Irregular Shapes of Water Clusters Generated in Supersonic Expansions. *Phys. Rev. Lett.* **2014**, *112*, No. 113401.
(46) Winter, B.; Weber, R.; Widdra, W.; Dittmar, M.; Faubel, M.; Hertel, I. V. Full Valence Band Photoemission from Liquid Water Using EUV Synchrotron Radiation. *J. Phys. Chem. A* **2004**, *108*, 2625−2632.
(47) Nishizawa, K.; Kurahashi, N.; Sekiguchi, K.; Mizuno, T.; Ogi, Y.; Horio, T.; Oura, M.; Kosugi, N.; Suzuki, T. High-resolution Soft X-ray Photoelectron Spectroscopy of Liquid Water. *Phys. Chem. Chem. Phys.* **2011**, *13*, 413−417.
(48) Kurahashi, N.; Karashima, S.; Tang, Y.; Horio, T.; Abulimiti, B.; Suzuki, Y.-I.; Ogi, Y.; Oura, M.; Suzuki, T. Photoelectron Spectroscopy of Aqueous Solutions: Streaming Potentials of NaX (X = Cl, Br, and I) Solutions and Electron Binding Energies of Liquid Water and X^-. *J. Chem. Phys.* **2014**, *140*, No. 174506.
(49) Perry, C. F.; Zhang, P.; Nunes, F. B.; Jordan, I.; von Conta, A.; Wörner, H. J. Ionization Energy of Liquid Water Revisited. *J. Phys. Chem. Lett.* **2020**, *11*, 1789−1794.
(50) Olivieri, G.; Goel, A.; Kleibert, A.; Cvetko, D.; Brown, M. A. Quantitative Ionization Energies and Work Functions of Aqueous Solutions. *Phys. Chem. Chem. Phys.* **2016**, *18*, 29506−29515.
(51) Pohl, M. N.; Muchová, E.; Seidel, R.; Ali, H.; Sršeň, Š; Wilkinson, I.; Winter, B.; Slavíček, P. Do Water's Electrons Care About Electrolytes. *Chem. Sci.* **2019**, *10*, 848−865.
(52) Nishitani, J.; Karashima, S.; West, C. W.; Suzuki, T. Surface Potential of Liquid Microjet Investigated Using Extreme Ultraviolet Photoelectron Spectroscopy. *J. Chem. Phys.* **2020**, *152*, No. 144503.
(53) Malerz, S.; Trinter, F.; Hergenhahn, U.; Ghrist, A.; Ali, H.; Nicolas, C.; Saak, C.-M.; Richter, C.; Hartweg, S.; Nahon, L.; et al. Low-Energy Constraints on Photoelectron Spectra Measured from Liquid Water and Aqueous Solutions. *Phys. Chem. Chem. Phys.* **2021**, *23*, 8246−8260.
(54) Perry, C. F.; Jordan, I.; Zhang, P.; von Conta, A.; Nunes, F. B.; Wörner, H. J. Photoelectron Spectroscopy of Liquid Water with Tunable Extreme-Ultraviolet Radiation: Effects of Electron Scattering. *J. Phys. Chem. Lett.* **2021**, *12*, 2990−2996.
(55) Gartmann, T. E.; Hartweg, S.; Ban, L.; Chasovskikh, E.; Yoder, B. L.; Signorell, R. Electron Scattering in Large Water Clusters from Photoelectron Imaging with High Harmonic Radiation. *Phys. Chem. Chem. Phys.* **2018**, *20*, 16364−16371.
(56) Saak, C.-M.; Richter, C.; Unger, I.; Mucke, M.; Nicolas, C.; Hergenhahn, U.; Caleman, C.; Huttula, M.; Patanen, M.; Björneholm, O. Proton Dynamics in Molecular Solvent Clusters as an Indicator for Hydrogen Bond Network Strength in Confined Geometries. *Phys. Chem. Chem. Phys.* **2020**, *22*, 3264−3272.
(57) Behrens, M.; Fröchtenicht, R.; Hartmann, M.; Siebers, J.-G.; Buck, U.; Hagemeister, F. C. Vibrational Spectroscopy of Methanol and Acetonitrile clusters in Cold Helium Droplets. *J. Chem. Phys.* **1999**, *111*, 2436−2443.
(58) Bradley, R. S.; Volans, P.; Whytlaw-Gray, R. Rates of Evaporation VI. The Vapour Pressure and Rate of Evaporation of Potassium Chloride. *Proc. R. Soc. London, Ser. A* **1953**, *217*, 508−523.
(59) Laria, D.; Fernández-Prini, R. Molecular Dynamics Study of Water Clusters Containing Ion Pairs: From Contact to Dissociation. *J. Chem. Phys.* **1995**, *102*, 7664−7673.
(60) Bondybey, V. E.; Beyer, M. K. How Many Molecules Make a Solution. *Int. Rev. Phys. Chem.* **2002**, *21*, 277−306.
(61) Sen, A.; Ganguly, B. What is the Minimum Number of Water Molecules Required to Dissolve a Potassium Chloride Molecule. *J. Comput. Chem.* **2010**, *31*, 2948−2954.
(62) Soper, A. K.; Weckström, K. Ion Solvation and Water Structure in Potassium Halide Aqueous Solutions. *Biophys. Chem.* **2006**, *124*, 180−191. Ion Hydration Special Issue.
(63) Jungwirth, P.; Tobias, D. J. Chloride Anion on Aqueous Clusters, at the Air-Water Interface, and in Liquid Water: Solvent Effects on Cl- Polarizability. *J. Phys. Chem. A* **2002**, *106*, 379−383.
(64) Zhao, Y.; Li, H.; Zeng, X. C. First-Principles Molecular Dynamics Simulation of Atmospherically Relevant Anion Solvation in Supercooled Water Droplet. *J. Am. Chem. Soc.* **2013**, *135*, 15549−15558.
(65) Cheng, M. H.; Callahan, K. M.; Margarella, A. M.; Tobias, D. J.; Hemminger, J. C.; Bluhm, H.; Krisch, M. J. Ambient Pressure X-ray Photoelectron Spectroscopy and Molecular Dynamics Simulation Studies of Liquid/Vapor Interfaces of Aqueous NaCl, RbCl, and RbBr Solutions. *J. Phys. Chem. C* **2012**, *116*, 4545−4555.
(66) Tissot, H.; Olivieri, G.; Gallet, J.-J.; Bournel, F.; Silly, M. G.; Sirotti, F.; Rochet, F. Cation Depth-Distribution at Alkali Halide Aqueous Solution Surfaces. *J. Phys. Chem. C* **2015**, *119*, 9253−9259.
(67) Stuart, S. J.; Berne, B. Surface Curvature Effects in the Aqueous Ionic Solvation of the Chloride Ion. *J. Phys. Chem. A* **1999**, *103*, 10300−10307.
(68) Sun, L.; Li, X.; Tu, Y.; Ågren, H. Origin of Ion Selectivity at the Air/Water Interface. *Phys. Chem. Chem. Phys.* **2015**, *17*, 4311−4318.
(69) Liu, J.; Zhang, J. Z. H.; He, X. Probing the Ion-Specific Effects at the Water/Air Interface and Water-Mediated Ion Pairing in Sodium Halide Solution with Ab Initio Molecular Dynamics. *J. Phys. Chem. B* **2018**, *122*, 10202−10209.
(70) Park, S.-C.; Pradeep, T.; Kang, H. Ionic Dissociation of NaCl on Frozen Water. *J. Chem. Phys.* **2000**, *113*, 9373−9376.
(71) Borodin, A.; Höfft, O.; Krischok, S.; Kempter, V. Ionization and Solvation of CsCl Interacting with Solid Water. *J. Phys. Chem. B* **2003**, *107*, 9357−9362.
(72) Kim, J.-H.; Shin, T.; Jung, K.-H.; Kang, H. Direct Observation of Segregation of Sodium and Chloride Ions at an Ice Surface. *ChemPhysChem* **2005**, *6*, 440−444.
(73) Kim, J.-H.; Kim, Y.-K.; Kang, H. Interaction of NaF, NaCl, and NaBr with Amorphous Ice Films. Salt Dissolution and Ion Separation at the Ice Surface. *J. Phys. Chem. C* **2007**, *111*, 8030−8036.
(74) Ahmed, M.; Apps, C.; Hughes, C.; Watt, N.; Whitehead, J. Adsorption of Organic Molecules on Large Water Clusters. *J. Phys. Chem. A* **1997**, *101*, 1250−1253.
(75) Pysanenko, A.; Habartová, A.; Svrčková, P.; Lengyel, J.; Poterya, V.; Roeselová, M.; Fedor, J.; Fárník, M. Lack of Aggregation of Molecules on Ice Nanoparticles. *J. Phys. Chem. A* **2015**, *119*, 8991−8999.
(76) Lietard, A.; Verlet, J. R. R. Selectivity in Electron Attachment to Water Clusters. *J. Phys. Chem. Lett.* **2019**, *10*, 1180−1184.
(77) Caleman, C.; van der Spoel, D. Temperature and Structural Changes of Water Clusters in Vacuum due to Evaporation. *J. Chem. Phys.* **2006**, *125*, No. 154508.
(78) Caleman, C.; van der Spoel, D. Evaporation from Water Clusters Containing Singly Charged Ions. *Phys. Chem. Chem. Phys.* **2007**, *9*, 5105−5111.
(79) Heiles, S.; Cooper, R. J.; DiTucci, M. J.; Williams, E. R. Sequential Water Molecule Binding Enthalpies for Aqueous Nanodrops Containing a Mono-, di- or Trivalent Ion and Between 20 and 500 Water Molecules. *Chem. Sci.* **2017**, *8*, 2973−2982.

https://doi.org/10.1021/acs.jpca.1c01539
J. Phys. Chem. A 2021, 125, 4750−4759

(80) Olleta, A. C.; Lee, H. M.; Kim, K. S. Ab initio Study of Hydrated Sodium Halides $NaX(H_2O)_{1-6}$ (X = F, Cl, Br, and I). *J. Chem. Phys.* **2006**, *124*, 024321.
(81) Olleta, A. C.; Lee, H. M.; Kim, K. S. Ab initio Study of Hydrated Potassium Halides $KX(H_2O)_{1-6}$ (X = F,Cl,Br,I). *J. Chem. Phys.* **2007**, *126*, No. 144311.
(82) Weber, R.; Winter, B.; Schmidt, P. M.; Widdra, W.; Hertel, I. V.; Dittmar, M.; Faubel, M. Photoemission from Aqueous Alkali-Metal-Iodide Salt Solutions Using EUV Synchrotron Radiation. *J. Phys. Chem. B* **2004**, *108*, 4729−4736.
(83) Dolgounitcheva, O.; Zakrzewski, V. G.; Ortiz, J. V. Electron Detachment Energies of Aqueous and Cluster Halide Anions from Electron Propagator Calculations with the Polarizable Continuum Model. *Int. J. Quantum Chem.* **2012**, *112*, 3840−3848.
(84) Gaiduk, A. P.; Govoni, M.; Seidel, R.; Skone, J. H.; Winter, B.; Galli, G. Photoelectron Spectra of Aqueous Solutions from First Principles. *J. Am. Chem. Soc.* **2016**, *138*, 6912−6915.
(85) Bouchafra, Y.; Shee, A.; Réal, F.; Vallet, V.; Severo Pereira Gomes, A. Predictive Simulations of Ionization Energies of Solvated Halide Ions with Relativistic Embedded Equation of Motion Coupled Cluster Theory. *Phys. Rev. Lett.* **2018**, *121*, No. 266001.
(86) Coons, M. P.; Herbert, J. M. Quantum Chemistry in Arbitrary Dielectric Environments: Theory and Implementation of Non-equilibrium Poisson Boundary Conditions and Application to Compute Vertical Ionization Energies at the Air/Water Interface. *J. Chem. Phys.* **2018**, *148*, No. 222834.
(87) DelloStritto, M.; Xu, J.; Wu, X.; Klein, M. L. Aqueous Solvation of the Chloride Ion Revisited with Density Functional Theory: Impact of Correlation and Exchange Approximations. *Phys. Chem. Chem. Phys.* **2020**, *22*, 10666−10675.
(88) Makov, G.; Nitzan, A. Solvation and Ionization near a Dielectric Surface. *J. Phys. Chem.* **1994**, *98*, 3459−3466.
(89) Winter, B.; Faubel, M. Photoemission from Liquid Aqueous Solutions. *Chem. Rev.* **2006**, *106*, 1176−1211.
(90) Arima, K.; Jiang, P.; Deng, X.; Bluhm, H.; Salmeron, M. Water Adsorption, Solvation, and Deliquescence of Potassium Bromide Thin Films on SiO_2 Studied by Ambient-Pressure X-ray Photoelectron Spectroscopy. *J. Phys. Chem. C* **2010**, *114*, 14900−14906.
(91) Winter, B.; Aziz, E. F.; Ottosson, N.; Faubel, M.; Kosugi, N.; Hertel, I. V. Electron Dynamics in Charge-Transfer-to-Solvent States of Aqueous Chloride Revealed by Cl- 2p Resonant Auger-Electron Spectroscopy. *J. Am. Chem. Soc.* **2008**, *130*, 7130−7138.
(92) Liu, J.; Zhang, H.; Li, Y.; Liu, Z. Disorder in Aqueous Solutions and Peak Broadening in X-ray Photoelectron Spectroscopy. *J. Phys. Chem. B* **2018**, *122*, 10600−10606.
(93) Ottosson, N.; Heyda, J.; Wernersson, E.; Pokapanich, W.; Svensson, S.; Winter, B.; Öhrwall, G.; Jungwirth, P.; Björneholm, O. The Influence of Concentration on the Molecular Surface Structure of Simple and Mixed Aqueous Electrolytes. *Phys. Chem. Chem. Phys.* **2010**, *12*, 10693−10700.
(94) Schläppi, B.; Ferreiro, J. J.; Litman, J. H.; Signorell, R. Sodium-sizer for Neutral Nanosized Molecular Aggregates: Quantitative Correction of Size-dependence. *Int. J. Mass Spectrom.* **2014**, *372*, 13−21.
(95) Björneholm, O.; Federmann, F.; Kakar, S.; Möller, T. Between Vapor and Ice: Free Water Clusters Studied by Core Level Spectroscopy. *J. Chem. Phys.* **1999**, *111*, 546−550.
(96) Abid, A. R.; Reinhardt, M.; Boudjemia, N.; Pelimanni, E.; Milosavljević, A. R.; Saak, C.-M.; Huttula, M.; Björneholm, O.; Patanen, M. The Effect of Relative Humidity on $CaCl_2$ Nanoparticles Studied by Soft X-ray Absorption Spectroscopy. *RSC Adv.* **2021**, *11*, 2103−2111.
(97) Pohl, M. N.; Richter, C.; Lugovoy, E.; Seidel, R.; Slavíček, P.; Aziz, E. F.; Abel, B.; Winter, B.; Hergenhahn, U. Sensitivity of Electron Transfer Mediated Decay to Ion Pairing. *J. Phys. Chem. B* **2017**, *121*, 7709−7714.

https://doi.org/10.1021/acs.jpca.1c01539
J. Phys. Chem. A 2021, 125, 4750−4759